Neuropharmacology 107 (2016) 201–214

Contents lists available at ScienceDirect

Neuropharmacology

journal homepage: www.elsevier.com/locate/neuropharm

SGIP1 alters internalization and modulates signaling of activated cannabinoid receptor 1 in a biased manner

Alena Hájková [a], Šárka Techlovská [a], Michaela Dvořáková [a], Jayne Nicole Chambers [a], Jiří Kumpošt [a], Pavla Hubálková [a], Laurent Prezeau [b], Jaroslav Blahos [a, *]

[a] Institute of Molecular Genetics, Academy of Science of the Czech Republic, Videnska 1083, 14220 Prague 4, Czech Republic
[b] Institut de Génomique Fonctionnelle, University of Montpellier 1 and 2, Montpellier, France

ARTICLE INFO

Article history:
Received 10 September 2015
Received in revised form
24 February 2016
Accepted 4 March 2016
Available online 9 March 2016

Keywords:
Seven transmembrane receptors
G-protein coupled receptors
Cannabinoid receptor 1
Protein-protein interactions
Bias signaling
Receptor endocytosis

ABSTRACT

Many diseases of the nervous system are accompanied by alterations in synaptic functions. Synaptic plasticity mediated by the endogenous cannabinoid system involves the activation of the cannabinoid receptor 1 (CB1R). The principles of CB1R signaling must be understood in detail for its therapeutic exploration. We detected the Src homology 3-domain growth factor receptor-bound 2-like (endophilin) interacting protein 1 (SGIP1) as a novel CB1R partner. SGIP1 is functionally linked to clathrin-mediated endocytosis and its overexpression in animals leads to an energy regulation imbalance resulting in obesity. We report that SGIP1 prevents the endocytosis of activated CB1R and that it alters signaling via the CB1R in a biased manner. CB1R mediated G-protein activation is selectively influenced by SGIP1, β-arrestin associated signaling is changed profoundly, most likely as a consequence of the prevention of the receptor's internalization elicited by SGIP1.

1. Introduction

Signaling via seven transmembrane receptors, also called G-protein coupled receptors (GPCRs), is tightly regulated by several mechanisms. These include post-translational modifications, the recruitment of β-arrestins, endocytosis and interactions with regulatory and scaffold proteins.

Cannabinoid receptor 1 (CB1R) is activated by endogenous cannabinoids (e.g. anandamide or 2-arachidonylglycerol), as well as by a range of exogenous ligands including -(−)-*trans*-Δ9-tetrahydrocannabinol (THC), the psychoactive compound found in the plant *Cannabis Sativa*. Localized principally presynaptically CB1R is abundant in many central nervous system (CNS) structures including the hypothalamus, hippocampus, nucleus accumbens, prefrontal cortex, cerebellum and the emetic centers in the brainstem. Activation of this receptor leads to attenuation of either inhibitory or excitatory synaptic transmission (Kano et al., 2009).

Like other GPCRs, CB1R regulates a diverse range of intracellular signaling pathways. The array of signals that are modified depends on the intrinsic properties of the ligands, the functional state of the receptors (secondary modifications, e.g. phosphorylation, ubiquitination etc.) and the intracellular environment (especially molecular components of signaling pathways and scaffold, together with regulatory proteins that are in close proximity). The G-protein signaling of CB1R leads to inhibition of adenylyl cyclase, negative modulation of various calcium channels, and activation of inwardly rectifying potassium channels. The extracellular signal-regulated

Abbreviations: SGIP1, src homology 3-domain growth factor receptor-bound 2-like (endophilin) interacting protein 1; CCP, clathrin-coated pit; AP2, assembly polypeptide 2; CB1R, cannabinoid receptor 1; CME, clathrin-mediated endocytosis; BRET, bioluminiscence resonance energy transfer; CNS, central nervous system; CHAPS, 3-[(3-cholamidopropyl)dimethylammonio]-1-propanesulfonate; CRIP1a, cannabinoid receptor-interacting protein 1a; DMSO, dimethyl sulfoxide; Eps15, epidermal growth factor receptor substrate 15; ERK 1/2, extracellular signal-regulated kinases1 and 2; FBS, fetal bovine serum; FCHo, Fer/Cip4 homology only proteins; FIR, fluorescence internalization ratio; FRET, Forster's resonance energy transfer; GPCRs, G-protein coupled receptors; HEK293, human embryonic kidney 293; MC, Mander's coefficient; PC, Pearson's coefficient; PTX, Pertussis toxin; Rluc, *Renilla* luciferase; Y2H, yeast two-hybrid; YFP, yellow fluorescent protein; WIN, WIN 55,212-2 mesylate, [(3R)-2,3-dihydro-5-methyl-3-(4-morpholinylmethyl)pyrrolo[1,2,3-de]-1,4-benzoxazin-6-yl]-1-naphthalenyl-methanone, monomethanesulfonate; AM281, 1-(2,4-Dichlorophenyl)-5-(4-iodophenyl)-4-methyl-*N*-4-morpholinyl-1*H*-pyrazole-3-carboxamide; CP55940, ((1R,3R,4R)-3-[2-hydroxy-4-(1,1-dimethylheptyl)phenyl]-4-(3- hydroxypropyl)cyclohexan-1-ol); ORG27569, (5-chloro-3-ethyl-1H-indole-2-carboxylic acid [2-(4-piperidin-1-yl-phenyl)ethyl] amide).

* Corresponding author.
E-mail address: blahos@img.cas.cz (J. Blahos).

http://dx.doi.org/10.1016/j.neuropharm.2016.03.008

kinases1 and 2 (ERK1/2) are activated in a G-protein dependent, or independent manner, in an agonist-specific way (Laprairie et al., 2014). Intracellular portions of the receptor play a crucial role in desensitization and internalization of the CB1R, a process related to the development of tolerance to agonists. Signaling of CB1R triggers activation of GPCR kinases or protein kinase C, resulting in receptor desensitization. Phosphorylation of two serine residues (S426, S430) within the C-terminus elicits receptor interaction with β-arrestins (Garcia et al., 1998; Morgan et al., 2014; Straiker et al., 2012). In heterologous cell systems, β-arrestin recruitment triggers a cascade of events resulting in the clathrin-mediated endocytosis (CME) of receptors (Hsieh et al., 1999). In addition to heterologous expression systems, rapid CB1R internalization is characteristic for the pool of CB1R located in the neuronal soma (Simon et al., 2013), while the CB1Rs in axons, and especially at synapses, are resistant to internalization (Leterrier et al., 2006; Mikasova et al., 2008; Stadel et al., 2011). The molecular mechanisms underlying these differences in endocytosis of the activated CB1Rs are unknown.

The carboxyl termini of GPCRs mediate multiple protein-protein interactions. Cannabinoid receptor-interacting protein 1a (CRIP1a) decreases CB1R Gαi/o mediated signaling. In addition, ERK1/2 signaling is attenuated in the presence of CRIP1a (Blume et al., 2015; Niehaus et al., 2007; Smith et al., 2015). To investigate the role of intracellular proteins affecting CB1R trafficking and signaling, we employed the yeast two-hybrid system (Y2H) to identify proteins that interact with the C-terminus of CB1R.

We identified the Src homology 3-domain growth factor receptor-bound 2-like (endophilin) interacting protein 1 (SGIP1) as a novel molecule associated with CB1R. We describe that SGIP1 interferes with CB1R internalization and influences its signaling in a biased manner, and may explain its dual internalization behavior in distinct neuronal compartments.

2. Methods

All chemicals were obtained from Sigma-Aldrich (Czech Republic), unless specified. All reagents for cell culture and transfection were purchased from Thermo Fisher Scientific Inc. (USA). WIN 55,212-2 mesylate (WIN) was obtained from Tocris R&D (USA) and 2-Arachidonoylglycerol (2-AG) and AM-281 from Cayman Chemicals (USA). Prior to making specific dilutions, a 10 mM stock was prepared in dimethyl sulfoxide (DMSO). The vehicle controls always contained appropriately diluted DMSO.

For primary neuronal cultures preparations, animals were treated in accordance to applicable local laws and were carried out in accordance with EU regulations. All efforts were made to minimize animal suffering, reduce the number of animals used and utilize alternatives to *in vivo* techniques, if available.

2.1. Expression vectors

The cDNA coding for mouse SGIP1 was purchased from TrueClones (Origene Technologies, Inc., USA), plasmids coding CB1R and CB1R N-terminal-GST fusion construct were kindly provided by Ken Mackie from Indiana University, Bloomington, Indiana, USA. Both full-length protein sequences were amplified using degenerate oligonucleotides for PCR, and inserted into pRK5 vector or pRK5 with a Flag-tag or YFP-tag. SNAP-tagged CB1R was generously provided by CisBio Bioassays (France). Expression vectors for Gqi9, β-arrestin1-Rluc, β-arrestin2-Rluc, $G\alpha_{i1}$-Rluc8, $G\alpha_{OA}$-Rluc8, Gβ-Flag, Gγ-VENUS and empty vector pRK6 have been described previously (Brule et al., 2014).

2.2. Yeast two-hybrid assay

All reagents for the yeast two-hybrid (Y2H) assay, yeast strains, plasmids and DNA library were purchased from Clontech Laboratories (Clontech Laboratories Inc., France) and handled according to the manufacturer's instructions. Identification of CB1R C-terminal (amino acids 420–473) interaction partners was performed with the MATCHMAKER Two-Hybrid System 3 according to the manufacturer's instructions. The CB1R bait was then cloned by PCR into the pGADT7 vector, transformed into the *Saccharomyces cerevisiae* strain AH109 and mated with pre-transformed Matchmaker rat forebrain *Saccharomyces cerevisiae* strain Y187 cDNA library. Mated cells were selected on SD media plates lacking Ade, His, Leu, Trp and containing X-Gal. Plasmid DNA was isolated from blue colonies and sequenced. For further interaction analyses, the carboxyl terminal of CB1R was mutated by site-directed mutagenesis. To confirm the originally identified interaction, we co-transformed both prey and bait vectors into the AH109 yeast strain by heat shock and grew them on SD/-Ade/-His/-Leu/-Trp/X-α-Gal media. This method was also used to test further interaction with the mutated CB1R C-terminus.

2.3. Cell culture and transfections

Human Embryonic Kidney 293 (HEK293) cells were cultured in Dulbecco's Modified Eagle's Medium (DMEM) containing glucose and L-glutamine supplemented with 10% fetal bovine serum (FBS) at 37 °C, 5% CO_2 and 95% humidity. Transient transfections were carried out either on 12 mm cover slips (Glaswarenfabrik Karl Hecht GMbH&Co KG, Germany) in 24 well plates (TPP, Switzerland) coated with poly-L-lysine or in 96 well plates (Greiner BioOne, UK) coated with poly-L-ornithine, using Lipofectamine™ 2000 according to the manufacturer's instructions. The total amount of DNA was kept at 800 ng/well (24 well) or 200 ng/well (96 well). Mock cells were transfected with an empty vector. Experiments were performed 24 h after transfection.

Rat embryonic cortical neurons E18 were isolated from Wistar rat brains and cultured as described previously (Brewer et al., 1993). Cell isolation was performed in Hank's Balanced Salt Solution (HBSS) supplemented with 10 mM HEPES (pH 7.0) and 0.25% Trypsin using Pasteur pipettes for tissue disruption. Approximately 750 cells/mm^2 were cultured on poly-L-lysine coated 18 mm cover slips in Neurobasal medium supplemented with B27, 0.5 mM L-glutamine and antibiotic mix.

2.4. Bioluminescence resonance energy transfer assay

To study the SGIP1-CB1R association, cells were transfected with SGIP1 N-terminally fused with Rluc (SGIP1-Rluc), and CB1R C-terminally fused with YFP (CB1R-YFP), while β-arrestin1 tagged N-terminally with YFP (β-arrestin1-YFP) was used as a negative control. For G-protein activation measurements, cells were transfected with tagged Gα, β, γ subunits together with CB1R-SNAP and Flag-SGIP1 or pRK6 (1:1:1:1:2). For β-arrestin recruitment experiments, cells were transfected with CB1R-YFP, β-arrestin1 or 2-Rluc and Flag-SGIP, DynK44A or pRK6, respectively (2:1:2). Transfected cells were washed twice with 150 μl PBS and coelentherazine h (Molecular Probes, USA) was added at a final concentration of 5 μM. Cells were stimulated with agonist or vehicle DMSO for the indicated time, or a few minutes after coelentherazine h addition in the G-protein activation experiment. Readings were performed immediately on a Mithras LB940 plate reader (Berthold Biotechnologies, Germany). The data are presented as specific BRET signal (net mBRET) calculated as the emission ratio 530 ± 25 nm/485 ± 20 nm × 1000 from cells transfected with both donor and

acceptor fusion proteins, minus the same ratio from cells transfected with an empty vector instead of the acceptor fusion protein. Data analyses were performed using Prism6 (GraphPad software, USA). For SGIP1-CB1R association YFP signal was measured in black plates at 535 nm ± 25 nm after excitation at 485 nm. Signal from cells transfected with pRK6 instead of the YFP fused constructs was subtracted and the specific YFP signal obtained was divided by the Rluc signal measured at 485 ± 20 nm.

2.5. Antibody production and characterization

We generated and characterized a novel serum in guinea pig against the synthetic peptide linked to thyroglobulin against the N-terminal SGIP1 epitope MMEGLKKRTRKAFGIRKKEKDTDSTGSC-COOH in the same manner as described previously (Techlovska et al., 2014). Protein samples for SDS-PAGE corresponding to 50 μg of cell lysate were separated on polyacrylamide Tris-glycine gel (10%). Separated proteins were transferred onto nitrocellulose membranes (Pall Corporation, USA). Membranes were blocked in 5% blotting-grade powdered milk (Carl Roth, Germany) and labeled with the following antibodies: primary anti-SGIP1 1:1000 and secondary goat anti-guinea pig IgG-HRP antibody (Santa Cruz Biotechnology, USA) 1:5000; primary mouse anti-Flag M2 antibody (Sigma-Aldrich, Czech Republic) 1:1000 and secondary goat anti-mouse IgG-HRP antibody (Promega, USA) 1:10 000; primary rabbit anti-actin antibody (Sigma-Aldrich, Czech Republic) 1:10 000 and secondary goat anti-rabbit IgG-HRP antibody (Promega, USA) 1:10 000. Samples were visualized using the SuperSignal West FEMTO chemiluminescent substrate system (Thermo Fisher Scientific, USA) and detected on the LAS-300 system (Fujifilm, USA).

In-house developed a-CB1R05 rabbit antibodies recognizing the N-terminus epitope fused to GST (a.a. residues 1–66) were used for co-immunoprecipitation studies. These a-CB1R05 antibodies were characterized for their specificity on immunoblots from both CB1R transfected HEK 293 cells and mock cells.

2.6. Detergent solubilization and co-immunoprecipitation

Previously described procedures were used with minor adjustments (Techlovska et al., 2014). Briefly, 20 μl of Protein A/G beads (Thermo Scientific) slurry was incubated with 1 μl a-CB1R05 sera overnight. The following day, mouse brain tissue was homogenized at 5 μg/μl total protein in buffer A (100 mM NaCl, 20 mM Tris; pH 7.4; with protease inhibitor cocktail tablet (Roche, USA)). In addition, 3-[(3-cholamidopropyl) dimethylammonio]-1-propanesulfonate (CHAPS) was added to the mix to a final concentration of 1%, incubated at 37 °C for 1 h and then centrifuged at 100,000× g for 1 hour. The supernatant was diluted (1:10) with buffer A containing 0.1% Triton X-100. Next, 1 ml of the diluted sample was mixed with the A/G beads bound with antibodies and rotated at 4 °C for 3–4 hours. The beads with bound fractions were then washed 3 times in buffer A containing 0.1% Triton X-100. The samples were then incubated with 50 μl of SDS-PAGE treatment buffer (0.25 M Tris-Cl, 8% SDS, 20% glycerol, 0.02% bromophenol blue, 0.04 M DTT, pH 6.8) for 10 minutes at 70 °C. Finally, 10 μl of each sample was resolved on SDS-PAGE, blotted onto nitrocellulose membrane and the immunoprecipitate/co-immunoprecipitate was visualized using corresponding antibodies.

2.7. Immunofluorescence labeling

Primary cortical neurons 9th day *in vitro* or transiently transfected HEK293 cells were fixed for 13 min in fresh 3% paraformaldehyde (Electron Microscopy Sciences, USA) diluted in Phosphate Buffered Saline (PBS). Fixed cells were permeabilized for 10 min in mild permeabilization buffer containing 0.025% Triton X-100, 0.05% Tween 20 and 1% bovine serum albumin (BSA) in PBS (pH 7.4). Primary antibodies were diluted in PBS containing 0.01 M Tris and 1% BSA (pH 7.4). Homemade affinity purified polyclonal antibodies: guinea pig anti-SGIP1 1:500, rabbit anti-Bassoon (KK06/A63) 1:2000 (kindly provided by Eckart D. Gundelfinger and Anna Fejtova from Leibniz Institute for Neurobiology, Germany) and commercial polyclonal rabbit anti-CB1R 1:200 (Alomone Labs, Israel), mouse monoclonal anti-MAP2 1:2000, mouse monoclonal anti-Tau1 (Millipore, Czech Republic) 1:500 and anti-Flag M2 antibody (Sigma Aldrich, Czech Republic) 1:500 were used for tandem staining of endogenous proteins as indicated. The secondary antibodies Alexa Fluor® 488 goat anti-rabbit IgG (H + L; Life Technologies, USA) 1:1000, Cy™3-conjugated Affini-Pure donkey anti-guinea pig IgG (H + L; Jackson ImmunoResearch, UK) 1:300 and C™5-conjugated Affini-Pure goat anti-mouse IgG (H + L; Millipore, Czech Republic) 1:300 were used according to manufacturer recommendations.

The modified live-cell immunofluorescence labeling protocol was used for immunofluorescence CB1R internalization assay in HEK293 cells (Lavezzari et al., 2004). Next, the cells were transiently transfected with CB1R and pRK6 (1:1) or CB1R and Flag-SGIP1 (1:1) constructs (total cDNA used was 800 ng/well in 24 well plates). After 24 h, the cells were incubated with rabbit anti-CB1R antibody (1:400) in complete cell culture medium at 37 °C for 2 h and then stimulated with 0.5 μM WIN 55,212-2 diluted in complete culture medium for 30 minutes at 37 °C before the standard fixation step (3% paraformaldehyde, 13 min, room temperature). Tandem staining with secondary antibodies was performed at room temperature with a saturated concentration of anti-rabbit antibodies in PBS for 45 minutes. First, Alexa Fluor® 488 goat anti-rabbit IgG (H + L; Life Technologies, USA) diluted 1:250 was employed, followed by the standard permeabilization step (see above) and application of Alexa Fluor® 633 goat anti-rabbit IgG (H + L; Life Technologies, USA) 1:250.

2.8. Image acquisition, processing and analysis

Microscope slides of fixed and labeled neurons were scanned on an inverted fluorescent microscope Leica DMI6000 with confocal extension Leica TCS SP5 AOBS TANDEM confocal superfast scanner; objective 63 × 1.4 oil (Leica Microsystems, Germany). Slides with HEK293 cells were scanned on an inverted fluorescence microscope Delta Vision Olympus IX-71; objective 60×/1.42 Plan APO N oil (Olympus, Japan). Deconvolution was performed using Huygens Software (Scientific Volume Imaging B.V., the Netherlands). The point spread function and chromatic aberration of the objective were determined by measurement of 100 nm beads. Further image analysis was performed using ImageJ (NIH, USA).

Co-localization analysis in neuronal cultures was performed from five regions of interest (ROIs) in each set of images by evaluating the co-localization of signals in different image channels acquired in these areas. We applied Pearson's (PC) and Mander's (MC) correlation coefficients mean values ($\bar{x}_{PC}$ and $\bar{x}_{MC}$) (Bolte and Cordelieres, 2006). The PC value ranges from 1 to −1, with 1 indicating for complete positive correlation, −1 for negative correlation and zero for no correlation. As PC values are dependent on noise, variations in fluorescence intensities and the type of fluorescence pattern, the MC coefficient was also applied to correlate co-localization of the channels based on an overlapping pixel pattern. This coefficient uses the average intensity values of two channels and values range from 0 to 1 proportionally corresponding to overlap (Lavezzari et al., 2004). As coefficients are sensitive to background levels, automatic Costes' approach was applied to separate image signal from the background (Costes et al., 2004).

CB1R internalization fluorescence mean density values S, I and B, corresponding to the cell surface CB1R labeled with Alexa 488 (S), the internalized CB1R labeled with Alexa 633 (I) and the background of images outside the cells (B) respectively, were measured using ImageJ. The background fluorescence B was subtracted from the S and I values, which, once multiplied by the respective areas, yielded the S* and I* total specific fluorescence (Leterrier et al., 2006). The fluorescence internalization ratio (FIR) was calculated as I*/S*. For each condition, eight cells from three independent experiments were used. Data were statistically analyzed using Prism6 (GraphPad software, USA).

2.9. Internalization assay

Levels of receptor internalization were determined by Forster's resonance energy transfer assay (FRET) as described previously (Maurel et al., 2008). The cells transfected with SNAP-CB1R and Flag-SGIP1 or DynK44A or pRK6 (1:2) were labeled with 100 nm SNAP-Lumi4Tb in Tag-lite labeling medium (CisBio bioassays, France). The level of receptor internalization was measured after 4 washes in Tag-lite labeling medium containing 24 μM fluorescein (Sigma Aldrich, Czech Republic) after cell stimulation with 2.5 μM WIN or DMSO using an Infinite F500 microplate reader (Tecan Group Ltd., Switzerland). Both donor emission signal at 520 ± 10 nm and FRET emission signal at 620 ± 10 nm were measured. Receptor internalization induced an increase in the donor signal over the FRET signal, which was calculated as donor emission signal/FRET emission signal × 10,000.

2.10. Intracellular calcium measurement

Intracellular calcium release was measured as described previously (Goudet et al., 2004). Subsequently, the cells were transfected with CB1R, Flag-SGIP1 and chimeric G-protein Gqi9 (1:2:1). After 24 h the cells were loaded with 1 μM Fluo4 AM for 1 h at 37 °C (Thermo Fisher Scientific, USA), washed and calcium release was measured after WIN stimulation. The change in fluorescence at 525 nm was measured for 60 s in 1.5 s intervals on a Multi-Mode Microplate Reader FlexStation 3 (Molecular Devices, USA). Dose-response curves were fitted using Prism6 (GraphPad software, USA).

2.11. Extracellular signal-regulated kinases 1/2 phosphorylation assay

The extent of extracellular signal-regulated kinases 1/2 (ERK1/2) phosphorylation was measured using a Phospho-ERK (Thr202/Tyr204) Cellular Assay Kit (CellulErk®, Cisbio Bioassays, France) as described previously (Brule et al., 2014). The cells transfected with SNAP-CB1R and Flag-SGIP1 or pRK6 (1:2) were serum-starved overnight, and 100 ng/ml of Pertussis toxin (Calbiochem, Czech Republic) was added when indicated. The stimulation was performed in DMEM (without FBS). The cells were kept in a incubator for the indicated stimulation time and then lysed immediately in 50 μl of supplemented lysis buffer. Sixteen μl of the lysate was then transferred into a 384-well small volume black plate (Greiner Bio One, UK) in duplicates and 2 μl of anti-Phospho-ERK1/2-d2 and Anti-ERK1/2-Eu^{3+}Cryptate antibodies were added. Fluorescence was read at 665 nm and 620 nm using a RUBYstar Time-Resolved Fluorescence Microplate Reader (BMG Labtechnologies, France). Data are presented as the ratio of 665/620 nm emission × 10,000. Dose-response curves were fitted using Prism6 (GraphPad software, USA). Statistical analysis was performed using the one-way ANOVA followed by Turkey's multiple comparison test (Prism6; GraphPad).

3. Results

3.1. Detection of SGIP1 as an interacting partner of CB1R

The yeast two-hybrid screen (Y2H) was employed to search for interacting partners of CB1R. The sequence corresponding to the C-terminal portion of CB1R following the 8th intracellular alpha-helix (amino acid residues 420–473) was used as bait against a cDNA library derived from rat forebrain. A sequence coding for the last 99 amino acids of the protein SGIP1 was detected as prey. The interaction between the CB1R C-terminus and the SGIP1 C-terminus was verified by re-transformation of both prey and bait coding vectors into the yeast strain AH109, which was grown on selection media lacking Ade, His, Leu, Trp and containing X-Gal. This allowed control of transcription activation of three reporter genes (His3, Ade2, Mel1) in parallel, reducing the incidence of false positive results.

This approach was also used for further investigation of CB1R/SGIP1 interaction, where serine and threonine residues were mutated to protonated glutamic or aspartic acid respectively, in order to mimic the potential phosphorylation that does not occur naturally in yeast, whereas in mammals CB1R undergoes C-terminal phosphorylation. None of these mutations had an effect on the interaction of the two peptides in our assay (Fig. 1A).

3.2. SGIP1 associates with CB1R

The association between SGIP1 and CB1R was verified *in vivo* using the co-immunoprecipitation technique. For immunoprecipitation, sera were selected from a set of antibodies made in-house against CB1R (not shown). To avoid co-migration of CB1R with the antibodies on immunoblots, HEK293 cells transfected with CB1R-GFP fusion protein were used. The selected a-CB1R05 antibodies were characterized and used for immunoprecipitation. Based on previous reports, 1% CHAPS was used for detergent solubilization. The selected a-CB1R05 serum was used to pull down detergent soluble protein. Irrelevant rabbit antibodies were used as a control. Next, the samples were resolved on SDS-PAGE and the immunoblots were probed with the novel antibodies raised against SGIP1.

The BRET approach was used to study the association of SGIP1 with CB1R in transfected HEK293 cells. SGIP1-Rluc construct contained N-terminally fused Renilla luciferase (Rluc), while CB1R-YFP was made as a C-terminal fusion protein. BRET titration curves revealed a large and saturated increase in BRET signal between SGIP1-Rluc and CB1R-YFP, both in the presence and absence of the agonist. In contrast, β-arrestin1-YFP, used as a negative control, produced only a small increase in BRET signal (Fig. 1B).

3.3. Characterization of antibodies

To detect SGIP1, antibodies were generated and characterized using SGIP1-transfected and non-transfected (mock) HEK293 cells prior to further studies. Immunofluorescent labeling of permeabilized cells and immunoblotting with resolved membranes from these cells were used (Fig. 2). Protein samples from the non-transfected cells showed no staining with our antibodies, indicating low background labeling of this antibody. This also suggests that HEK293 cells do not endogenously express SGIP1, as cells transfected with Flag-tagged SGIP1 were strongly stained with a pattern suggesting membrane-associated molecules. Moreover, the N-terminally located Flag-epitope was also labeled in a similar pattern (Fig. 2A). HEK293 cell (mock or Flag-SGIP1 transfected) membranes were detected with antibodies recognizing SGIP1 and Flag-tag to test the selectivity of the novel SGIP1 antibody. A single band with

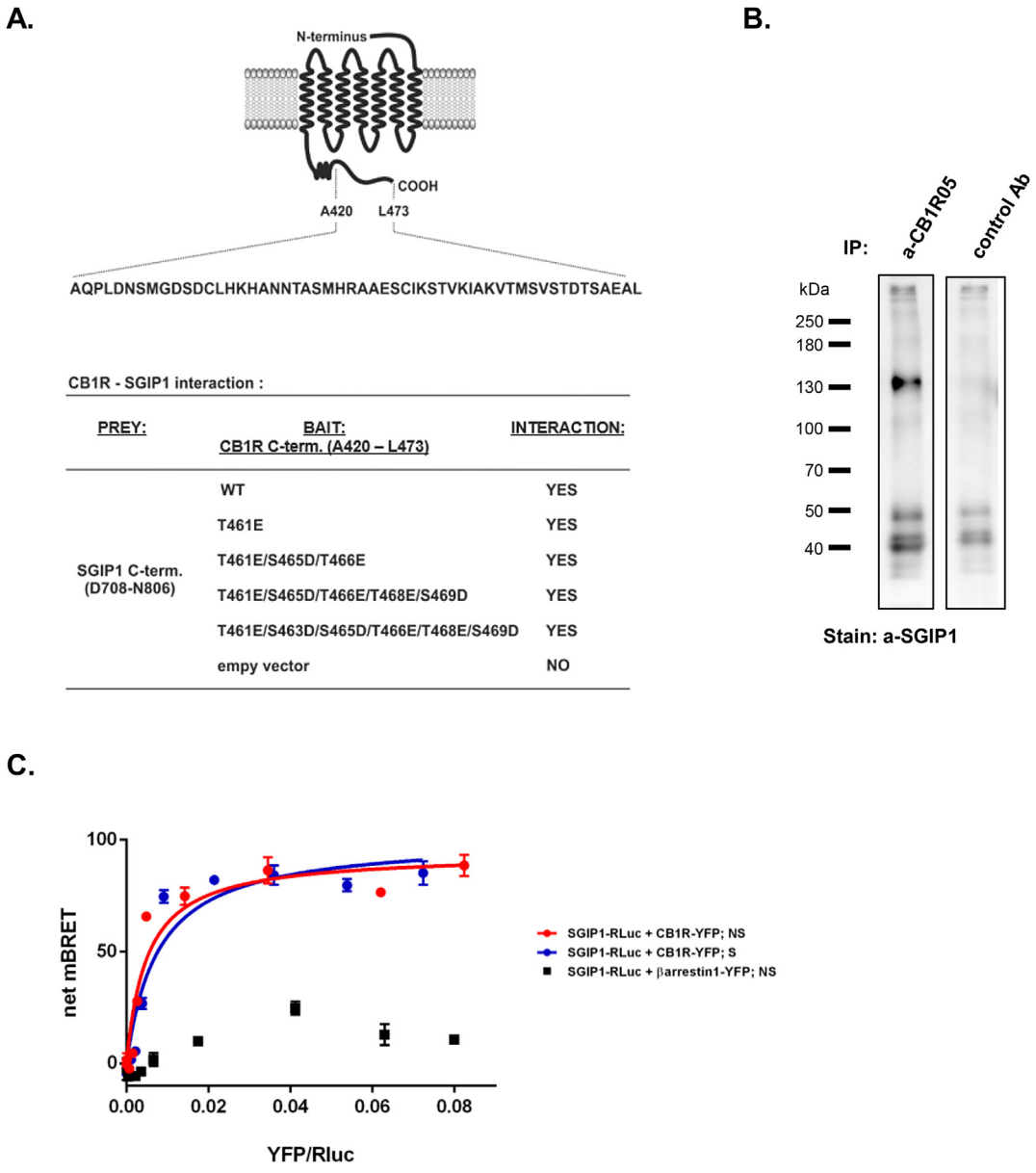

CB1R - SGIP1 interaction :

PREY:	BAIT: CB1R C-term. (A420 – L473)	INTERACTION:
SGIP1 C-term. (D708-N806)	WT	YES
	T461E	YES
	T461E/S465D/T466E	YES
	T461E/S465D/T466E/T468E/S469D	YES
	T461E/S463D/S465D/T466E/T468E/S469D	YES
	empy vector	NO

Fig. 1. Yeast-two hybrid analysis. A) Schematic representation of CB1R – SGIP1 interaction by Y2H analysis. SGIP1 interaction with CB1R identified upon Y2H screening against the rat forebrain cDNA library was further verified by re-transforming both prey and bait constructs into the yeast strain AH109 and growing on selective media to confirm the interaction. Further analysis of potential phosphorylation sites modification on the interaction was performed using a series of CB1R baits in which the indicated threonine and serine residues were mutated to the protonated states to mimic their phosphorylation. B) Co-immunoprecipitation of SGIP1 with CB1R from the CHAPS soluble fraction of rat brain homogenates. C) BRET titration curves of HEK293 cells transiently co-transfected with constant amount of SGIP1-Rluc and increasing amount of CB1R-YFP or β-arrestin1-YFP. Cells were stimulated with 2.5 μM WIN (S) 5 min before BRET was measured after a coelantherazine-h (5 μM) addition. NS represents non-stimulated cells.

the expected weight of the Flag-SGIP protein (approximately 100 kDa) was recognized by both the SGIP1 antibodies and Flag antibodies. Therefore, the antibodies were found to be suitable for further studies (Fig. 2B). Similarly, mock and CB1R expressing cells were used to characterize the a-CB1R05 antibodies used for immunoprecipitation (Fig. 2C).

3.4. SGIP1 and CB1R co-localize in neurites

To determine whether the two molecules co-localize in the same subcellular compartments, immunolabeling of CB1R and SGIP1 was performed in primary neuronal cultures.

The SGIP1 protein co-localized with the axonal marker Tau1 as well as with anti-Bassoon antibodies, which label presynaptic portions of the neurites. Overlap in SGIP1 and Bassoon staining was observed. Co-localization of SGIP1 with the dendritic marker MAP2 only partially overlapped and we concluded that SGIP1 labeling is found on the presynaptic portions of afferent neurites. SGIP1 was found to be present (at least partially) in neuronal compartments in which CB1R was detected. Employing CB1R specific antibodies together with SGIP1 detection showed an overlapping punctuated pattern in MAP2-negative structures that corresponded to the presynaptic portions observed in anti-Bassoon labeling (Fig. 3A and B).

Co-localization was quantified from five cropped regions of interest (ROIs) (Fig. 3B), expressed as Pearson's (PC) and Mander's (MC) correlation coefficients mean values (Fig. 3C). Presynaptic targeting of CB1R correlated with mean PC ($\bar{x}_{PC} = 0.20$; SD = 0.06) and MC ($\bar{x}_{MC} = 0.49$; SD = 0.03) values obtained for CB1/MAP2

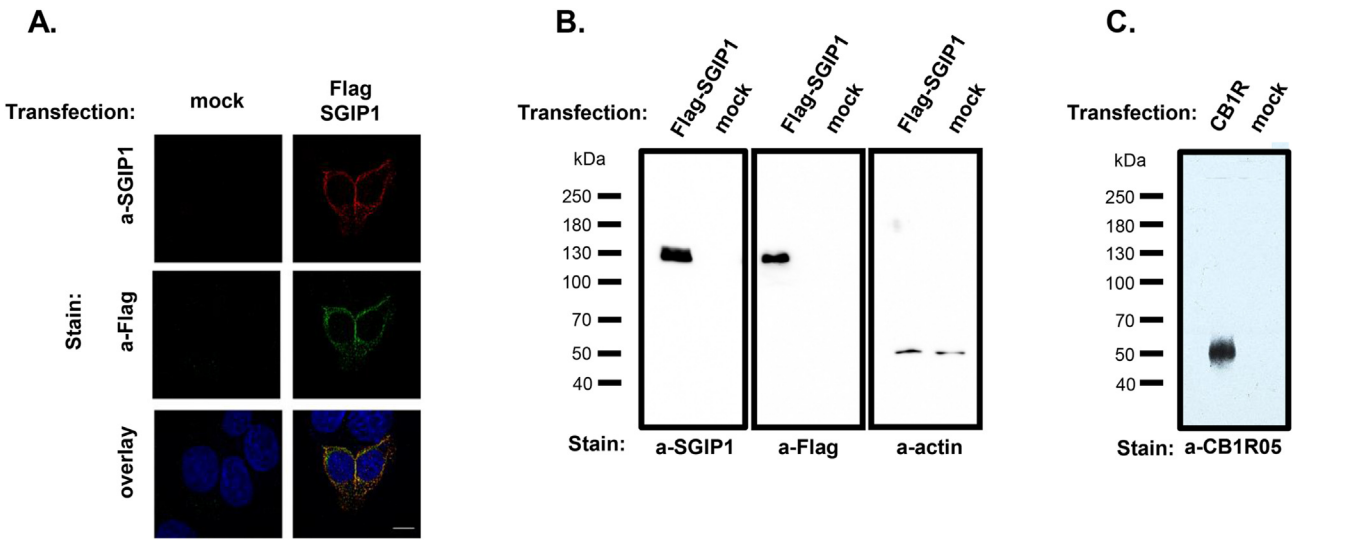

Fig. 2. Characterization of anti-SGIP1 and anti-CB1 antibodies. A) HEK293 cells were transfected with pRK6 (mock) or Flag-SGIP1, fixed, permeabilized and stained with anti-SGIP1 (SGIP1) and anti-Flag (Flag) antibodies as indicated. Images are Maximum Intensity projections of 5 stacks (z = 0.25 μm). Scale bar = 10 μm. B) Characterization of the anti-SGIP antibody by Western blot. HEK293 cells were transfected with Flag-SGIP1 or pRK6 (mock). Cell lysates were separated by SDS-PAGE and then subjected to Western blotting. Membranes were stained either with anti-SGIP1 (SGIP1), anti-Flag (Flag) or anti-Actin (actin) antibodies as indicated. C) Anti-CB1R antibody characterization. Transfected HEK293 cells with CB1R coding expression vector and mock cells were resolved on SDS-PAGE and stained using antibodies.

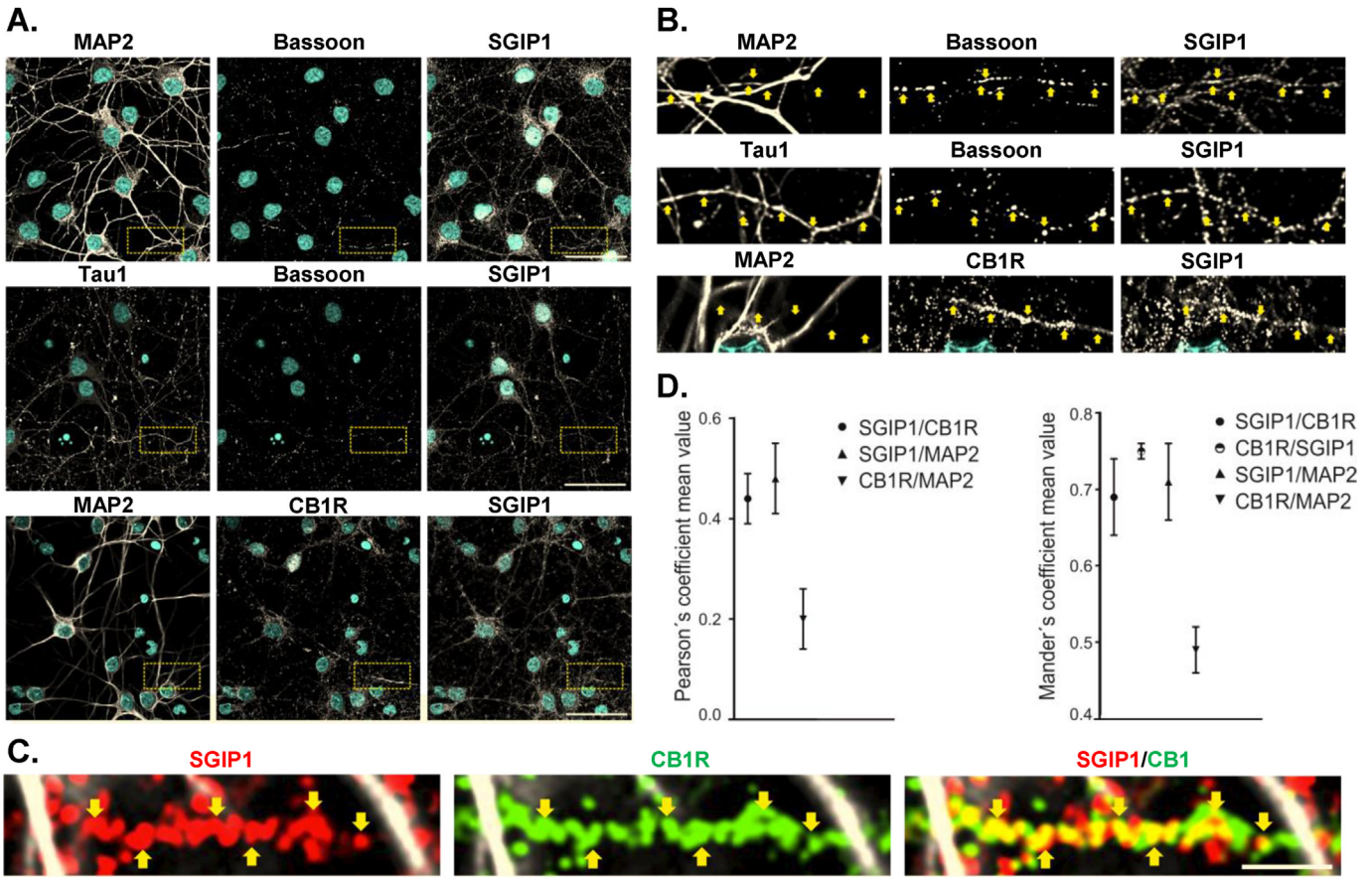

Fig. 3. Co-localization of SGIP1 with compartment-specific neuronal markers and CB1R in cultured cortical neurons A) Specific neuronal compartments were labeled by dendritic (MAP2), axonal (Tau1), and presynaptic terminal (Bassoon) markers in cultured cortical neurons. The localization of the markers, SGIP1 and CB1R is shown. Scale bar = 20 μm. B) Cropped images from the yellow ROIs in A. Specific neuronal structures are indicated with yellow arrows, where the punctuated signal of SGIP1 and CB1R was detected. C) Dual-channel cropped images representing the overlap of two labeled proteins. Endogenous SGIP is always represented by intensities in the red channel, the green channel expresses endogenous CB1R signal and the grey channel corresponds to MAP2 labelling. Scale bar = 1 μm. D) Statistical analysis of overlapping pixel intensities in dual-channel images of CB1R and SGIP1 or both proteins separately with MAP2 from regions corresponding to detail cropped images on left side were performed and expressed as Pearson's (PC) and Mander's (MC) coefficient mean values (C) shown in the graphs.

overlap. The homogenous fluorescence pattern of dendrites labeled by MAP2 contrasted with the punctuated fluorescence observed with CB1R and SGIP1 that share a similar fluorescence pattern (Fig. 3B). SGIP1 is not strictly targeted to presynaptic portions due to higher PC and MC mean values ($\bar{x}_{PC}$ = 0.48, SD = 0.07; $\bar{x}_{MC}$ = 0.71; SD = 0.05) obtained for SGIP/MAP2. Nevertheless, the mean value of CB1R/SGIP1 ($\bar{x}_{MC}$ = 0.75; SD = 0.01) indicates stronger co-localization of CB1 with SGIP1 than obtained for SGIP/MAP2 ($\bar{x}_{MC}$ = 0.71; SD = 0.05) and SGIP1/CB1R ($\bar{x}_{MC}$ = 0.69, SD = 0.05).

3.5. SGIP1 impedes endocytosis of activated CB1R

The TR-FRET based method was used to investigate whether SGIP1 interaction with CB1R influences internalization of the activated receptor, as reported for other cargoes (Uezu et al., 2007). With this method, the fluorescence signal of benzyl guanidine-cryptate-labeled N-terminally tagged SNAP-CB1R at the cell surface is quenched by the fluorescein dye present in the medium at a high concentration (24 μM). An increase in donor signal is related to internalization of the receptor, as the signal is not quenched by extracellular fluorescein. Significant CB1R internalization after both 5 μM 2-AG and 2.5 μM WIN stimulation in HEK293 cells expressing CB1R alone was observed. Both agonists initiated prompt and massive internalization of comparable pace and extent. Interestingly, when CB1R was co-expressed with SGIP1, agonist induced endocytosis was significantly reduced (percentage of maximal CB1R internalization after WIN stimulation ± SEM, where mean internalization of CB1R alone was set to 100 %: CB1R_2-AG = 100 ± 3.4%; CB1R + SGIP1_2-AG = 29.1 ± 0.12% and CB1R_WIN = 100 ± 1.6%; CB1R + SGIP1_WIN = 30.2 ± 0.37%, n = 3, *P ˂ 0.0001) (Fig. 4A).

The dominant negative dynamin mutant K44A (DynK44A) has previously been shown to block clathrin-coated pit (CCP) mediated endocytosis. DynK44A was used to elucidate the mechanism of SGIP1 interference with CB1R endocytosis. The inhibitory effect of DynK44A on WIN mediated CB1R internalization was greater (CB1R + DynK44A = 9.2 ± 1.3%, n = 3) than when SGIP1 was co-transfected (see above).

SGIP1 also affected CB1R internalization without agonist addition. Such internalization was quantitatively lower that one elicited by high doses of agonists in the absence of SGIP1, but was also almost diminished by the presence of SGIP1. As expected, the inverse agonist 1-(2,4-Dichlorophenyl)-5-(4-iodophenyl)-4-methyl-*N*-4-morpholinyl-1H-pyrazole-3-carboxamide (AM281) did interfere with the internalization of CB1R observed without agonist treatment. However, it had no apparent effect on internalization of CB1R expressed in tandem with SGIP1, as the internalization was prevented by the presence of SGIP1 (Fig. 4B). As this assay measures the fluorescence signal of the intracellular pool of receptors, the different fluorescence profiles measured in cells with and without SGIP1 show that the internal pool of receptors is smaller in the presence of SGIP1. Conversely, surface expression levels in non-stimulated cells were comparable in cells expressing CB1R alone, in tandem with SGIP1, or with DynK44A (Fig. 4C).

The results of agonist driven internalization were confirmed using live-cell immunofluorescence labeling of the HEK293 cells transfected with CB1R with or without SGIP1 (Fig. 4D). Prior to activation, anti-CB1R antibody was used for staining cell surface exposed receptors. After stimulation with WIN or DMSO (30 minutes), cells were treated with an excessive amount of two different secondary antibodies. Primarily applied secondary antibody labeled the extracellular CB1R epitopes. After permeabilization, another secondary antibody with a different fluorophore recognized the internalized pool of CB1R. CB1R internalization was calculated as the ratio between the internalized pool and cell surface CB1R staining. Following WIN stimulation, CB1R internalization was significantly decreased in the presence of SGIP1 compared to CB1R alone (FIR ± SEM values for CB1R = 2.139 ± 0.18; CB1R + SGIP1 = 0.642 ± 0.24; n = 8; *P ˂ 0.0001).

3.6. β-arrestin2 association with activated CB1R is enhanced by SGIP1

β-arrestins are adaptor molecules that interact with desensitized GPCRs, endocytic machinery molecules and specific signaling cascade molecules. The BRET based assay was used to measure cells co-expressing β-arrestin1-Rluc or β-arrestin2-Rluc and CB1R-YFP, where an increase of BRET signal reflected the recruitment of β-arrestin by the receptor upon either 5 μM 2-AG or 2.5 μM WIN treatment. No associations elicited by either agonist between CB1R and β-arrestin1, with or without SGIP1, were observed.

In cells expressing CB1R without SGIP1, the β-arrestin2-Rluc/CB1R-YFP signal reached its maximum 5 min after the application of either of the two agonists and decreased to basal levels within an hour, although the effect mediated by 2-AG was much lower than that of WIN (Fig. 5). In cells co-expressing SGIP1, the dynamics of the association between CB1R and β-arrestin2 after WIN stimulation was reminiscent of that without SGIP1, with culmination in 5 min, but BRET efficiency reached considerably higher values and persisted for an extended time. Therefore SGIP1 profoundly affects the interaction between CB1R and β-arrestin2 (net mBRET values ± SEM in 5 minutes: CB1R = 36.9 ± 2.8; CB1R + SGIP1 = 54 ± 0.9; n = 3). The effect was even higher in cells co-transfected with CB1R and DynK44A (net mBRET value ± SEM in 5 minutes: CB1R + DynK44A = 64 ± 1.2; n = 3).

3.7. SGIP1 does not interfere with CB1R mediated G-protein activation

To test whether CB1R signaling via Gi/Go activation is affected by SGIP1, a G-alpha BRET-based sensor was used to monitor conformational changes between alpha and gamma G-protein subunits. Both Gi/Go activations mediated by CB1R stimulation were tested with increasing concentrations of WIN. In both cases, activation of the receptor was followed by a prompt decrease in BRET signal efficiency, reflecting activation of the G-proteins (Fig. 6A). These changes were similar when measured in cells transfected with CB1R alone or together with SGIP1 for the tested G-subunits ($logEC_{50}$ ± SEM for Gi activation: CB1R = −7.5 ± 0.1 nM; CB1R + SGIP1 = −7.5 ± 0.1 nM; Go activation: CB1R = −7.4 ± 0.1 nM; CB1R + SGIP1 = −7.5 ± 0.1 nM, n = 3).

The measurement of intracellular calcium release was assessed using co-transfection with the chimeric G-protein Gqi9. Intracellular calcium was measured as an increase in fluorescence in transiently transfected HEK293 cells loaded with Fluo-4 dye. No significant differences in CB1R-Gqi9 mediated calcium mobility with or without SGIP1 were observed ($logEC_{50}$ ± SEM values: CB1R WIN = −6.7 ± 0.1 nM; CB1R + SGIP1 2-AG = −6.7 ± 0.1 nM; CB1R 2-AG = −6.2 ± 0.3 nM; CB1R + SGIP1 2-AG = −6 ± 0.3 nM) upon either 2-AG or WIN mediated activation. These results suggest that acute G-protein signaling of CB1R elicited by a single-dose of either agonist is not markedly influenced by SGIP1 (Fig 6B).

3.8. SGIP1 alters ERK1/2 signaling of CB1R

The role of SGIP1 on ERK1/2 signaling following CB1R activation was also investigated. In HEK293 cells transiently expressing CB1R ERK1/2 phosphorylation was induced by adding 5 μM 2-AG (Fig. 7A). The time course of ERK1/2 phosphorylation upon CB1R

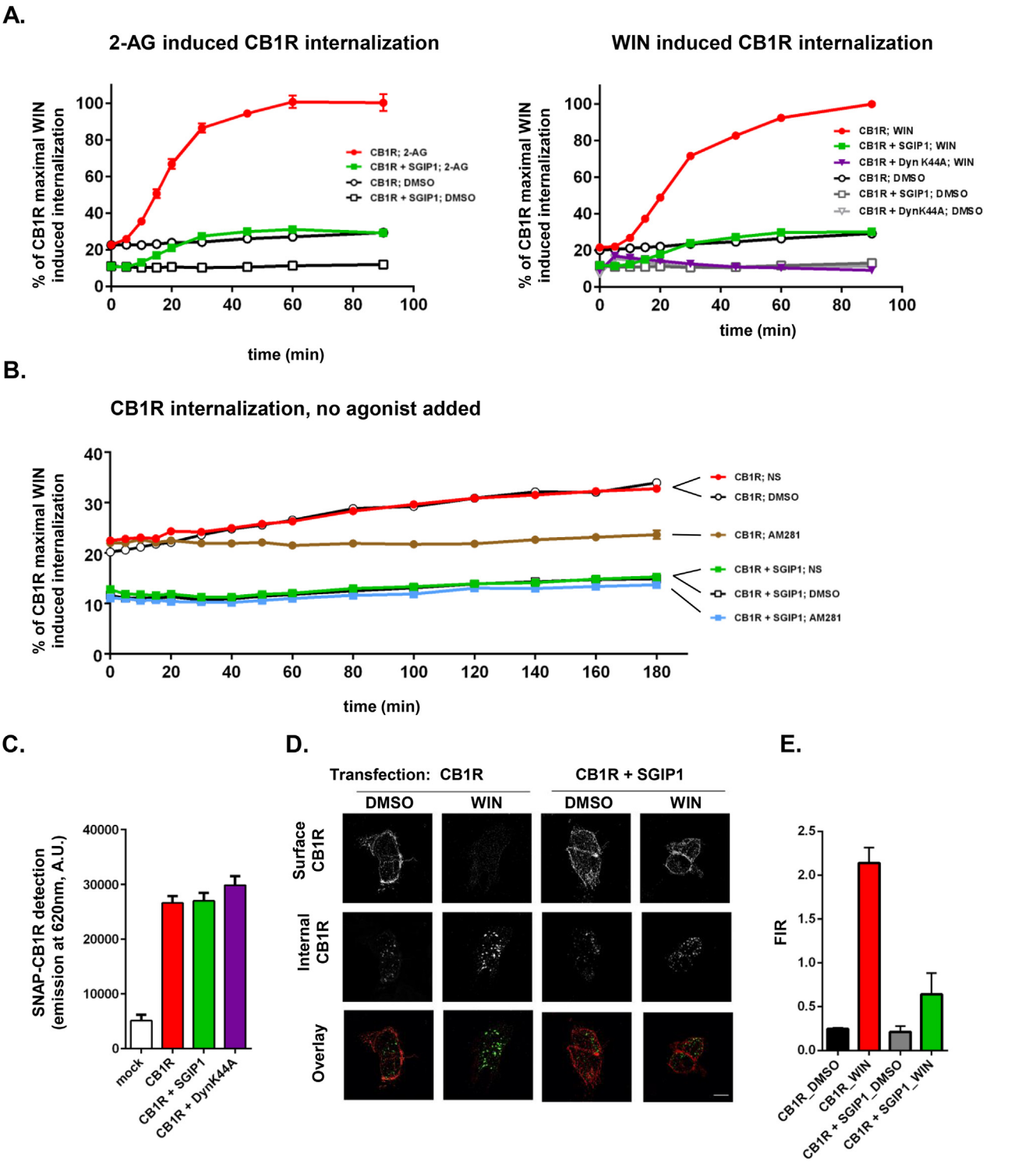

Fig. 4. SGIP1 interferes with internalization of activated CB1R. A) HEK293 cells were transiently transfected with SNAP tagged CB1R together with DynK44, Flag-SGIP1 or an empty vector respectively. The level of CB1R internalization was measured after 5 μM 2-AG or 2.5 μM WIN stimulation at indicated times. The relative level of receptor internalization is calculated as the percentage ratio of the maximal internalization measured for CB1R alone after 5 μM 2-AG or 2.5 μM WIN stimulation respectively. The data represent means ± SEM of quadruplicates from a single experiment. Two further experiments produced similar results. B) The extent of CB1R internalization was also measured without agonist addition as well as with 7 μM inverse agonist AM-281 in cells transfected, as above. C) CB1R expression level determination. The SNAP-CB1R expression vector was transiently transfected alone or in tandem with Flag-SGIP1 or DynK44A into the HEK293 cells. After 24 h, the SNAP tag was labeled with benzyl guanine carrying europium cryptate (BG-K) and its emission signal reflecting the amount of surface CB1R was measured at 620 nm on an Infinite F500 microplate reader. D) HEK293 cells were transfected with CB1R or CB1R + SGIP1 and stimulated with 0.5 μM WIN (or DMSO as a control) for 30 minutes. Images shown are Z-projections of maximal intensity. The red color represents surface CB1R while green represents internalized CB1R. Scale Bar 10 μm. E) Graph showing the fluorescence internalization ratio (FIR), calculated as the ratio between the internalized and cell surface CB1R. Each value represents mean ± SEM (n = 8). Significant difference was determined using an unpaired t-test, P ˂ 0.0001.

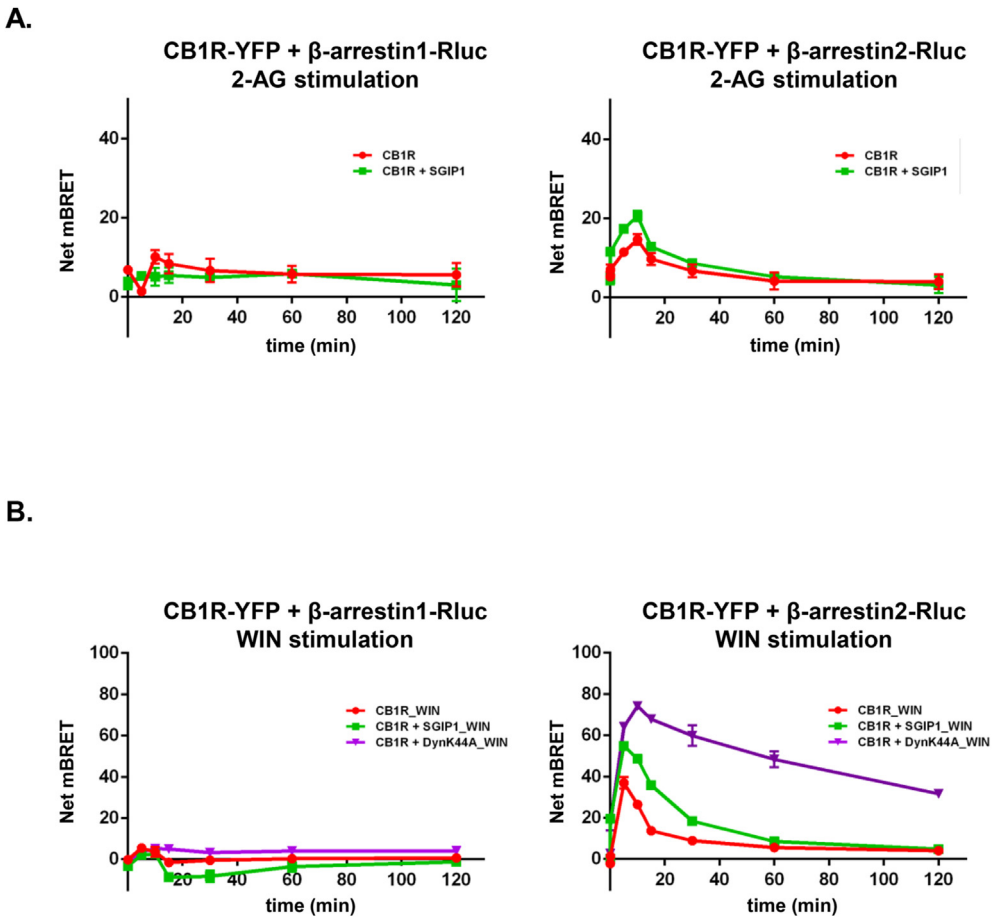

Fig. 5. β-arrestin2 association with activated CB1R is enhanced by SGIP1. HEK293 cells were transiently transfected with a particular β-arrestin-Rluc variant together with CB1R-YFP and with Flag-SGIP1 or DynK44A. Cells were stimulated with 5 μM (pannel A) 2-AG or 2.5 μM WIN (panel B) for the indicated time, and after the addition of 5 μM coelantherazine-h the BRET signal was measured on a Mithras LB940 plate reader. Data represent the mean ± SEM from three independent experiments performed in triplicate.

activation was transiently elevated with the maximal signal observed at around 5 min after agonist application. The maximal response and overall levels of ERK1/2 phosphorylation for the tested agonists were noticeably lower in cells co-expressing SGIP1 and the CB1R. We performed statistical analysis using the one-way ANOVA followed by Turkey's multiple comparison test for the responses in cells treated with 2-AG at peak response. There was a significant increase ($P < 0.0001$, $n = 7$) in ERK1/2 phosphorylation when CB1 was expressed alone compared to vehicle (DMSO) stimulation. There was also a significant difference ($P < 0.0001$, $n = 7$) between the effect mediated by 2-AG on CB1R when expressed alone or in tandem with SGIP1.

Treatment of 2.5 μM WIN (Fig. 7B, left) led to greater responses compared to 2-AG. SGIP1 also led to depression of the responses. Co-expression with DynK44A resulted in decreased ERK1/2 signaling similar to that observed with SGIP1, however the signal was more delayed and persisted for a longer period with DynK44A. Pre-treatment of the cells with Pertussis toxin (PTX) abolished the activated-CB1R-induced ERK1/2 phosphorylation in cells expressing CB1R alone and in cells co-expressing CB1R with SGIP1 as well (Fig. 7B, right).

The dose-response experiment measured after 5 min of 2.5 μM WIN stimulation (Fig. 7C) confirmed lower ERK1/2 phosphorylation levels mediated by stimulated CB1R upon co-expression with SGIP1, while the EC_{50} values remained comparable ($logEC_{50} \pm SEM$ values: CB1R = −6.9 ± 0.05 nM; CB1R + SGIP1 = −6.9 ± 0.05 nM; CB1R + DynK44A = −6.8 ± 0.08 nM, n = 3).

4. Discussion

We report the functional consequences of association between CB1R and SGIP1. The interaction was detected using Y2H (Fig. 1A) and confirmed by co-precipitation from detergent soluble of brain and also using the BRET approach (Fig. 1C). The proximity of SGIP1 and CB1R detected by BRET was not influenced by the presence or absence of the CB1R agonist WIN. As a control molecule, we chose β-arrestin1, which does not interact with non-activated CB1R. As expected, our results show that β-arrestin1 does not interact with SGIP1.

In rodents, SGIP1 is expressed almost exclusively in the CNS (Trevaskis et al., 2005). The pattern of expression of mRNAs for both, SGIP1 and CB1R, as documented in Allen's Brain Atlas, is largely overlapping, but expression levels seem to vary in different brain regions and cell types (http://mouse.brain-map.or, 2015; Lein et al., 2007). Detailed study of co-localization of the two proteins in various cell types and subcellular compartments, especially in respect to pre-synaptic distribution, deserves investigation on nanoscale level, as in recent elegant study on CB1R detection and its redistribution upon chronic THC exposures (Dudok et al., 2015).

We verified the co-localization of CB1R and SGIP1 in cultured neurons derived from prefrontal cortex. We observed strong co-localization of SGIP1 with axonal (Tau1) and presynaptic (Bassoon) markers. The pattern of partial co-localization with the dendritic marker MAP2 reflects the distribution of SGIP1 in pre-synaptic terminals (Fig. 3). Thus, SGIP1 is preferentially targeted to

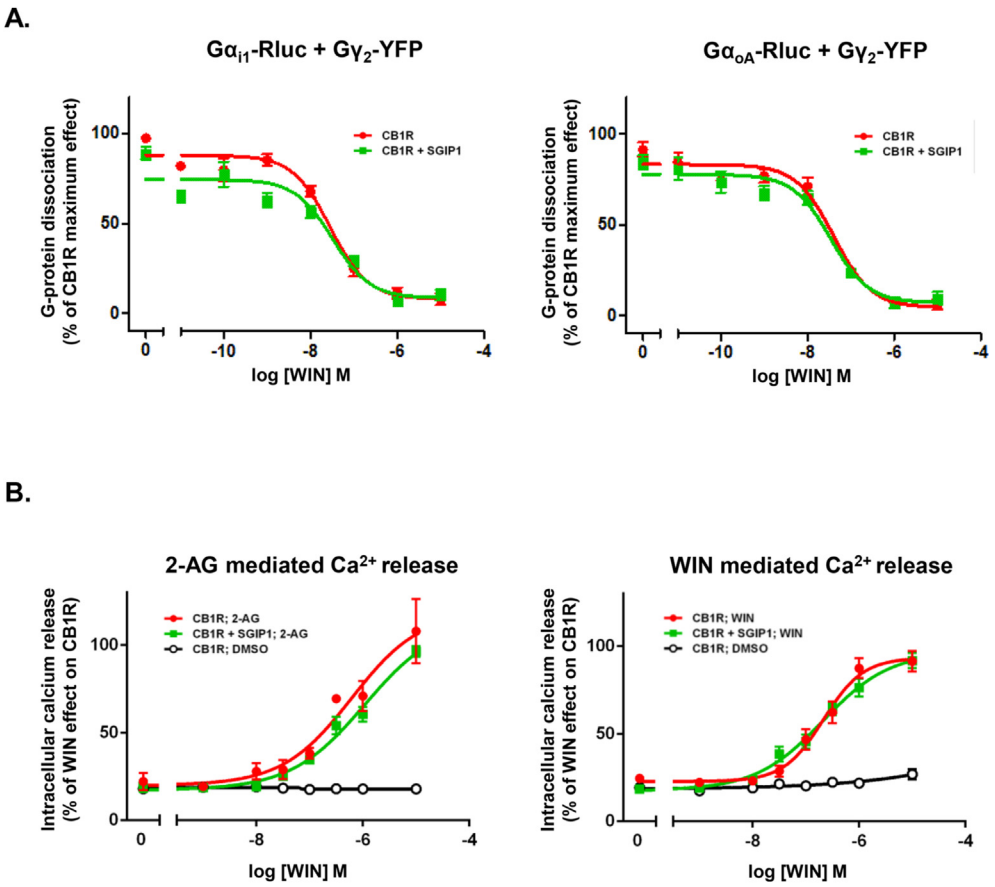

Fig. 6. SGIP1 does not significantly change CB1R mediated G-protein activation. A) Dose response curves of Gα subunit dissociation from the G-protein complex after CB1R stimulation with increasing concentrations of WIN. HEK293 cells were simultaneously transiently co-transfected with $G\alpha_{i1}$-Rluc8 or $G\alpha_{oA}$-Rluc8, $G\beta_2$-Flag, $G\gamma_2$-VENUS, CB1R, and SGIP1 or an empty vector. Twenty-four hours after transfection, 5 μM coelantherazine-h was added, cells were stimulated with increasing concentrations of WIN and the decrease in BRET signal due to dissociation of the Gα subunit from the G-protein complex was measured. B) CB1R mediated intracellular calcium mobilization in response to stimulation with various concentrations of 2-AG or WIN. HEK293 cells were transiently transfected with CB1R, chimeric G-protein Gqi9 and Flag-SGIP1 or an empty vector. Cells were loaded with Fluo-4 and calcium release was measured. Data represent the mean ± SEM of three independent experiments performed in triplicate.

axons and presynaptic buttons. This corresponds to recently published findings identifying SGIP1 as a highly abundant presynaptic protein (Wilhelm et al., 2014).

It has been shown previously that SGIP1 decreases the rate of endocytosis of receptors that do not belong to the GPCR family (Uezu et al., 2007). We discovered that SGIP1 confers cell surface stability of the activated CB1R in co-transfected HEK293 cells and also blocks internalization of the receptor that occurs without any added agonists (Fig. 4). This sheds light on the possible machinery and may explain discrepancies reported in heterologous systems where significant CB1R internalization was observed and observations in neuronal cell bodies where limited internalization of CB1R located in presynaptic regions was observed (Straiker et al., 2012; Hsieh et al., 1999; Leterrier et al., 2006; Jin et al., 1999). Recent study on chronic THC treatment revealed, that diminishing of CB1R is cell-type specific. Thus, among others, it remains to be specified on nanoscale level, whether SGIP1 expression differs, for example, between GABAergic and glutamatergic synapses in hippocampus (Dudok et al., 2015). We did follow only acute internalization patterns of CB1R with and without SGIP1. Further studies using transgenic animals might resolve the *in vivo* situation following chronic THC treatment in respect with SGIP1 effect on CB1R signaling in distinct cell populations.

WIN-mediated activation of CB1R was shown to cause β-arrestin2, but not β-arrestin1 recruitment to the activated receptors (Daigle et al., 2008). SGIP1 enhanced association with β-arrestin2 upon activation with WIN or the endocannabinoid 2-AG. This finding excluded the possibility that decreased rates of activated CB1R internalization may be caused by SGIP1 competition with β-arrestins binding to the phosphorylated C-terminus of CB1R. No detectable interaction of β-arrestin1 with or without SGIP1 upon activation with WIN or 2-AG was detected (Fig. 5). Phosphorylated states of certain threonine and serine residues of the C-terminal region of CB1R precede the recruitment of β-arrestin2 to CB1R. In our Y2H experiments, we showed that mutation of these residues (and others) which mimic their phosphorylated states do not influence the interaction between SGIP1 and CB1R. (Fig. 1). Alteration of CB1R endocytosis by DynK44A changed the association with β-arrestin2 to a larger extent than SGIP1 (Fig. 5B). DynK44A blocks endocytosis at the latest steps of membrane invagination, prior to the scission of CCP, just before the formation of the vesicle and entrance into the cytoplasm, while SGIP1 probably interferes with the initial stages of CME.

A possible explanation for the SGIP1 mediated enhancement of β-arrestin2 association with CB1R is a lack of CB1R/β-arrestin2 complex sequestration that would occur upon receptor internalization and post-endocytic processing (see proposed model in Fig. 8) (Shukla et al., 2011; Luttrell and Gesty-Palmer, 2010; Shenoy et al., 2009; Tohgo et al., 2003; Pierce et al., 2000). Another possibility is that the recruitment of β-arrestin2 to the activated and

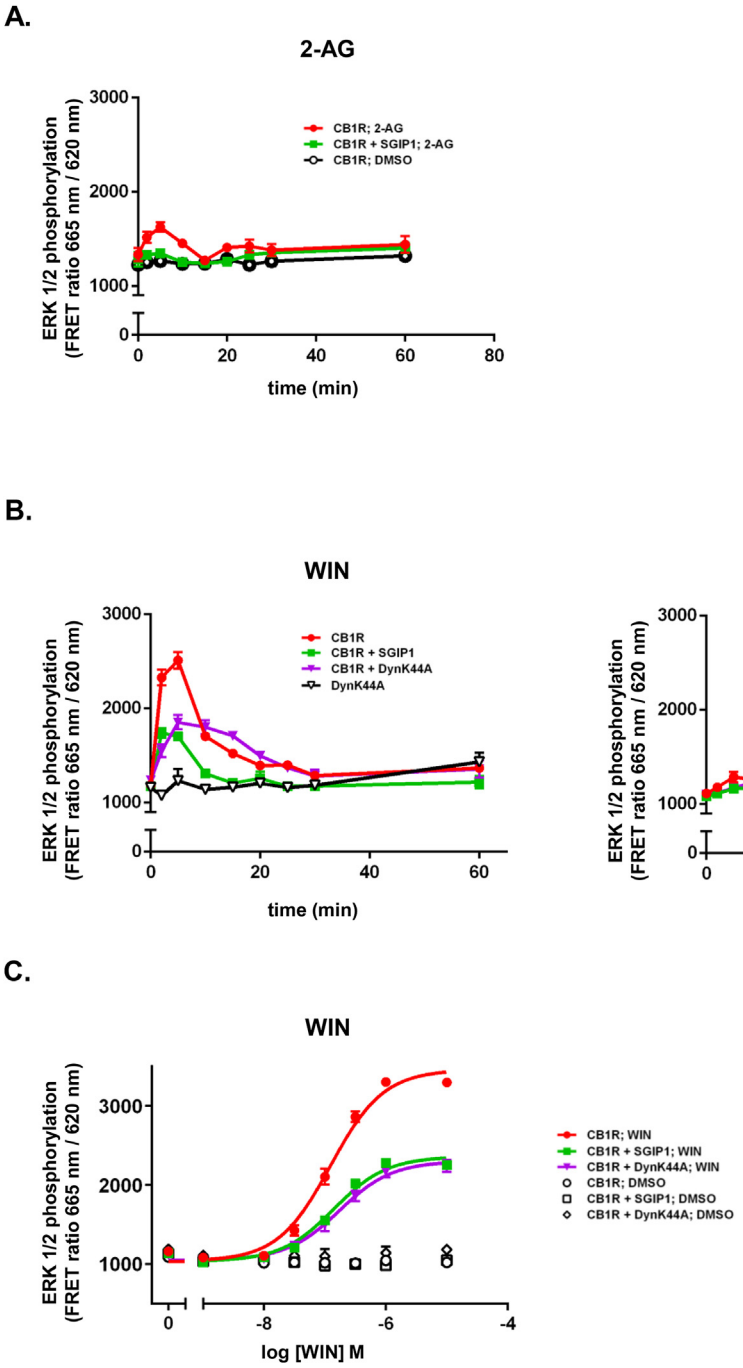

Fig. 7. CB1R mediated ERK1/2 signaling is hindered by SGIP1. HEK293 cells were transiently transfected with CB1R and co-transfected with either DynK44A or Flag-SGIP1 or an empty vector. The kinetics of CB1R mediated ERK1/2 phosphorylation were measured after addition of 5 μM 2-AG (panel A). Evaluation was performed after 5 minutes of stimulation. There was a significant difference between CB1R alone stimulated with 2-AG or DMSO ($P < 0.0001$, $n = 7$) and between the 2-AG effect on CB1R alone or in tandem with SGIP1 ($P < 0.0001$, $n = 7$). B) ERK1/2 activation using synthetic ligand WIN without (left), or after PTX pretreatment (right) C) Dose response curves of ERK 1/2 phosphorylation mediated via WIN stimulated CB1R alone or in tandem with SGIP1 or DynK44A. Data represent the mean ± SEM of three independent experiments performed in triplicate with the exception of the 2-AG stimulation for 0–30 minutes where seven independent experiments in triplicate were performed.

phosphorylated CB1R results in a different conformation of the arrestin molecule in the presence or absence of SGIP1 (Shukla et al., 2008).

SGIP1, together with the membrane-curvature-associated FCH domain only proteins FCHo1 and FCHo2 (FCHo1/2), belongs to the muniscin family that are involved in CME. While FCHo1/2 proteins have been shown to be involved in sustaining or promoting the initial phases of CME (Cocucci et al., 2012; Henne et al., 2010; Traub and Wendland, 2010), SGIP1 was shown to prevent the internalization of several cargoes (Uezu et al., 2007). The overall structure of the muniscins consists of the N-terminal lipid-binding domain, followed by protein-protein interaction mediating modules: AP2 binding site, a proline-rich region that occupies the central part of the polypeptide and the C-terminal part known as medium μ-domain of adaptor proteins (Henne et al., 2010; Hollopeter et al., 2014). These domains participate in the formation of intracellular

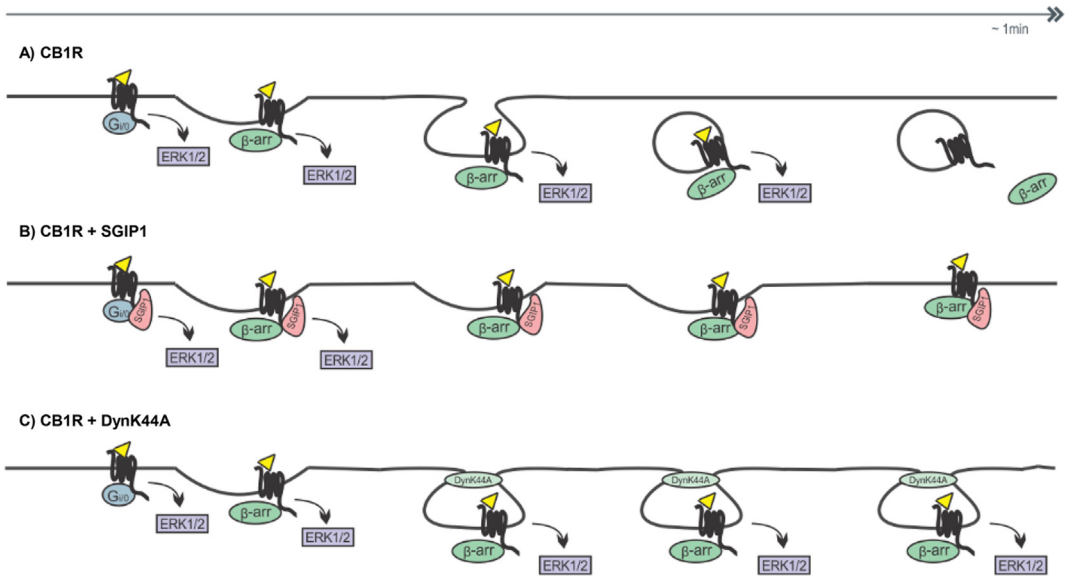

Fig. 8. Proposed model of SGIP1 effect on CB1R internalization and signaling. A) Transfected cells without SGIP1. Upon CB1R agonist induced signaling through Gi/o, the receptor associates with β-arrestin and is readily internalized, which allows massive ERK1/2 activation. B) In cells expressing SGIP1, internalization is prevented at the early stages. Therefore, G-protein signaling is unaltered. However, the extent of CB1R signaling via the ERK1/2 pathway is decreased, as SGIP1 competes with FCHo1/2 proteins required for the initial stages of clathrin-coated pit formation. Thus, the internalization of CB1R is abrupt at the early stage, when the pits are in the initial phases of growth, or even before this event. SGIP1 prevents ERK1/2 signaling of the receptor-β-arrestin complex that would occur during further steps of internalization. Conversely, β-arrestin association with CB1R is enhanced as their dissociation, which normally occurs in internalized endocytic compartments, does not occur. C) Blockade of endocytosis in later stages. DynK44A hinders CB1R internalization at the stage of endocytosis prior to scission of the clathrin coated pits. We assume that at this stage, the effect on signaling via ERK1/2 already proceeds and is extended, compared to the situation with SGIP1 or the receptor alone that internalizes, which leads to β-arrestin dissociation. This corresponds to the finding that DynK44A elevates CB1R- β-arrestin association.

transport vesicles and selection of cargo molecules. A novel motif on SGIP1 adjacent to the membrane interacting domain was recently identified for the clathrin adaptor protein complex AP2. Its interaction with the corresponding motif on FCHo1/2 results in AP2 activation (Hollopeter et al., 2014). Thus, another part of the SGIP1 molecule has to overcome AP2 activation. Such a motif may be the 97 amino acid residue N-terminal region, which was shown to interact with plasma membrane lipids.

We hypothesize that SGIP1 interferes with endocytosis by competition with FCHo1/2 proteins. FCHo1/2 have the N-terminal portion folded to form F-Bar domains that are responsible for plasma membrane shaping in CME pit formation (Henne et al., 2007), while the MP region of SGIP1 has no sequence similarity to these F-Bar structures. The most appealing hypothesis is that the MP region of SGIP1 interacts with the membrane in a different manner than FCHo1/2.

The association between SGIP1 and CB1R, as well as the resulting interference with the internalization of the activated receptor, has specific consequences on CB1R signaling. The activation of Gαi1 and GαoA proteins was measured as a change in BRET efficiency between Gα and Gγ subunits and dose response measurements using the Gαqi9 fusion protein in a Ca^{++} mobility assay. The results showed no significant difference in the activation of the G-proteins by the CB1 receptor in the presence or absence of SGIP1 (Fig. 6). Conversely, we found that CB1R elicited ERK1/2 phosphorylation was profoundly altered by SGIP1. The extent of ERK1/2 phosphorylation was reduced substantially by SGIP1, while the kinetic profile of ERK1/2 activation mediated by CB1R upon 2-AG or WIN application was comparable in the presence and absence of SGIP1 (Fig. 7).

ERK1/2 activation with or without SGIP1 was abolished in our experiments by PTX treatment. PTX did abolish ERK1/2 signaling elicited by CP55940 ((1R,3R,4R)-3-[2-hydroxy-4-(1,1-dimethylheptyl)phenyl]-4-(3-hydroxypropyl)cyclohexan-1-ol), but was not abolished when allosteric modulator ORG27569 (5-chloro-3-ethyl-1H-indole-2-carboxylic acid [2-(4-piperidin-1-yl-phenyl)ethyl]amide) was used in previous report (Ahn et al., 2012). This suggests that ERK1/2 signaling is dependent on Gαi-protein activation, that would elicit corresponding downstream signaling using WIN or CP55940, but distinct downstream signaling by G-protein Coupled Receptors Kinases activation takes place in presence of ORG27569 (Ahn et al., 2013). These findings parallel data from studies including situation in neuronal cells, where WIN stimulated CB1R mediated PTX sensitive ERK1/2 phosphorylation (Baillie et al., 2013; Dalton and Howlett, 2012).

DynK44A was also employed in the functional tests. In the presence of DynK44A, CB1R mediated ERK1/2 activation reached the same maximal levels as it did with SGIP1, but for a longer duration suggesting internalization and signaling during post-endocytic sorting of the receptor plays an important role in ERK1/2 signalization (see proposed model in Fig. 8) (Daaka et al., 1998).

Signaling bias was recognized for GPCR ligands that are likely to promote or stabilize specific conformations of their heptahelical domains. Novel molecules that adjust GPCR signaling by mechanisms other than the ligand-dependent stabilization of specific conformations were also developed; e.g., peptides derived from sequences of the intracellular loops connecting transmembrane alpha-helices (Quoyer et al., 2013). Also, single-domain antibodies (nanobodies), which are directed against intracellular regions of receptors, stabilized it in its active or inactive state (Staus et al., 2014). The intrinsic modulator of CB1R signaling, pregnenolone, acting as an allosteric biased signaling modulator, was shown to act as an ERK1/2-pathway specific inhibitor, leaving CB1R G-protein coupling unmodified (Wilhelm et al., 2014). Interestingly, SGIP1 elicits a similar effect on CB1R signaling as pregnenolone, however, the mechanism of this bias is likely different. Pregnenolone was proposed to interact with CB1R in a region constituted by α helices (Vallee et al., 2014), while we identified the SGIP1 interaction site

on the extreme C-tail following the 8th α-helix.

SGIP1 overexpression *in vivo* is associated with energy misbalance and obesity in animals (Trevaskis et al., 2005) and genetic variations within the SGIP1 gene are associated with energy balance disturbances in humans (Cummings et al., 2012). If the CB1R signaling pathway(s) affected in obese individuals could be pharmacologically influenced separately from the pathways involved in mental safeguarding well-being, then safer and more effective anti-obesity drugs could be developed. Only after the signaling pathway of CB1R in the obesity phenotype has been elucidated can specific antagonists, or partial agonists be developed while minimizing adverse effects such as those reported for Rimonabant. This anti-obesity drug was withdrawn from the market after evaluation of the risk-benefit ratio due to its severe psychiatric side effects. Pharmacological characterization of CB1R ligands on CB1R signaling has thus far been performed mostly in heterologous systems, in the absence of SGIP1. Therefore, further investigation into the signaling properties of the receptor and the effects of the molecular components of the signalosome on its properties are needed.

Conflicts of interest

The authors claim no conflict of interest.

Acknowledgements

We acknowledge the Microscopy Centre, IMG AS, Prague, Czech Republic for their support with obtaining the data presented in this paper, especially Ondrej Horvath and Ivan Novotny for help with image acquisition and Martin Capek for computational processing of the images and their statistical analysis. Pharmacological experiments were performed using the ARPEGE Pharmacology Screening- Interactome platform facility at the Institute of Functional Genomics (Montpellier, France).

We also thank Silvia Radenkovic for help with the manuscript preparation. The study was supported by the Czech Science Foundation (GACR P303/12/2408) and institutionally by RVO: 68378050.

References

Ahn, K.H., Mahmoud, M.M., Kendall, D.A., 2012. Allosteric modulator ORG27569 induces CB1 cannabinoid receptor high affinity agonist binding state, receptor internalization, and Gi protein-independent ERK1/2 kinase activation. J. Biol. Chem. 287, 12070–12082.

Ahn, K.H., Mahmoud, M.M., Shim, J.Y., Kendall, D.A., 2013. Distinct roles of beta-arrestin 1 and beta-arrestin 2 in ORG27569-induced biased signaling and internalization of the cannabinoid receptor 1 (CB1). J. Biol. Chem. 288, 9790–9800.

Baillie, G.L., Horswill, J.G., Anavi-Goffer, S., Reggio, P.H., Bolognini, D., Abood, M.E., McAllister, S., Strange, P.G., Stephens, G.J., Pertwee, R.G., Ross, R.A., 2013. CB(1) receptor allosteric modulators display both agonist and signaling pathway specificity. Mol. Pharmacol. 83, 322–338.

Blume, L.C., Eldeeb, K., Bass, C.E., Selley, D.E., Howlett, A.C., 2015. Cannabinoid receptor interacting protein (CRIP1a) attenuates CB1R signaling in neuronal cells. Cell. Signal. 27, 716–726.

Bolte, S., Cordelieres, F.P., 2006. A guided tour into subcellular colocalization analysis in light microscopy. J. Microsc. 224, 213–232.

Brewer, G.J., Torricelli, J.R., Evege, E.K., Price, P.J., 1993. Optimized survival of hippocampal neurons in B27-supplemented Neurobasal, a new serum-free medium combination. J. Neurosci. Res. 35, 567–576.

Brule, C., Perzo, N., Joubert, J.E., Sainsily, X., Leduc, R., Castel, H., Prezeau, L., 2014. Biased signaling regulates the pleiotropic effects of the urotensin II receptor to modulate its cellular behaviors. FASEB J. Off. Publ. Fed. Am. Soc. Exp. Biol. 28, 5148–5162.

Cocucci, E., Aguet, F., Boulant, S., Kirchhausen, T., 2012. The first five seconds in the life of a clathrin-coated pit. Cell 150, 495–507.

Costes, S.V., Daelemans, D., Cho, E.H., Dobbin, Z., Pavlakis, G., Lockett, S., 2004. Automatic and quantitative measurement of protein-protein colocalization in live cells. Biophys. J. 86, 3993–4003.

Cummings, N., Shields, K.A., Curran, J.E., Bozaoglu, K., Trevaskis, J., Gluschenko, K., Cai, G., Comuzzie, A.G., Dyer, T.D., Walder, K.R., Zimmet, P., Collier, G.R., Blangero, J., Jowett, J.B., 2012. Genetic variation in SH3-domain GRB2-like (endophilin)-interacting protein 1 has a major impact on fat mass. Int. J. Obes. 36, 201–206.

Daaka, Y., Luttrell, L.M., Ahn, S., Della Rocca, G.J., Ferguson, S.S., Caron, M.G., Lefkowitz, R.J., 1998. Essential role for G protein-coupled receptor endocytosis in the activation of mitogen-activated protein kinase. J. Biol. Chem. 273, 685–688.

Daigle, T.L., Kearn, C.S., Mackie, K., 2008. Rapid CB1 cannabinoid receptor desensitization defines the time course of ERK1/2 MAP kinase signaling. Neuropharmacology 54, 36–44.

Dalton, G.D., Howlett, A.C., 2012. Cannabinoid CB1 receptors transactivate multiple receptor tyrosine kinases and regulate serine/threonine kinases to activate ERK in neuronal cells. Br. J. Pharmacol. 165, 2497–2511.

Dudok, B., Barna, L., Ledri, M., Szabo, S.I., Szabadits, E., Pinter, B., Woodhams, S.G., Henstridge, C.M., Balla, G.Y., Nyilas, R., Varga, C., Lee, S.H., Matolcsi, M., Cervenak, J., Kacskovics, I., Watanabe, M., Sagheddu, C., Melis, M., Pistis, M., Soltesz, I., Katona, I., 2015. Cell-specific STORM super-resolution imaging reveals nanoscale organization of cannabinoid signaling. Nat. Neurosci. 18, 75–86.

Garcia, D.E., Brown, S., Hille, B., Mackie, K., 1998. Protein kinase C disrupts cannabinoid actions by phosphorylation of the CB1 cannabinoid receptor. J. Neurosci. Off. J. Soc. Neurosci. 18, 2834–2841.

Goudet, C., Gaven, F., Kniazeff, J., Vol, C., Liu, J., Cohen-Gonsaud, M., Acher, F., Prezeau, L., Pin, J.P., 2004. Heptahelical domain of metabotropic glutamate receptor 5 behaves like rhodopsin-like receptors. Proc. Natl. Acad. Sci. U. S. A. 101, 378–383.

Henne, W.M., Kent, H.M., Ford, M.G., Hegde, B.G., Daumke, O., Butler, P.J., Mittal, R., Langen, R., Evans, P.R., McMahon, H.T., 2007. Structure and analysis of FCHo2 F-BAR domain: a dimerizing and membrane recruitment module that effects membrane curvature. Structure. 15, 839–852.

Henne, W.M., Boucrot, E., Meinecke, M., Evergren, E., Vallis, Y., Mittal, R., McMahon, H.T., 2010. FCHo proteins are nucleators of clathrin-mediated endocytosis. Science 328, 1281–1284.

Hollopeter, G., Lange, J.J., Zhang, Y., Vu, T.N., Gu, M., Ailion, M., Lambie, E.J., Slaughter, B.D., Unruh, J.R., Florens, L., Jorgensen, E.M., 2014. The membrane-associated proteins FCHo and SGIP are allosteric activators of the AP2 clathrin adaptor complex. eLife 3.

Hsieh, C., Brown, S., Derleth, C., Mackie, K., 1999. Internalization and recycling of the CB1 cannabinoid receptor. J. Neurochem. 73, 493–501.

http://mouse.brain-map.org., A. I. f. B. S. A. M. B. A. I. A. f. (2015).

Jin, W., Brown, S., Roche, J.P., Hsieh, C., Celver, J.P., Kovoor, A., Chavkin, C., Mackie, K., 1999. Distinct domains of the CB1 cannabinoid receptor mediate desensitization and internalization. J. Neurosci. Off. J. Soc. Neurosci. 19, 3773–3780.

Kano, M., Ohno-Shosaku, T., Hashimotodani, Y., Uchigashima, M., Watanabe, M., 2009. Endocannabinoid-mediated control of synaptic transmission. Physiol. Rev. 89, 309–380.

Laprairie, R.B., Bagher, A.M., Kelly, M.E., Dupre, D.J., Denovan-Wright, E.M., 2014. Type 1 cannabinoid receptor ligands display functional selectivity in a cell culture model of striatal medium spiny projection neurons. J. Biol. Chem. 289, 24845–24862.

Lavezzari, G., McCallum, J., Dewey, C.M., Roche, K.W., 2004. Subunit-specific regulation of NMDA receptor endocytosis. J. Neurosci. Off. J. Soc. Neurosci. 24, 6383–6391.

Lein, E.S., Hawrylycz, M.J., Ao, N., Ayres, M., Bensinger, A., Bernard, A., Boe, A.F., Boguski, M.S., Brockway, K.S., Byrnes, E.J., Chen, L., Chen, L., Chen, T.M., Chin, M.C., Chong, J., Crook, B.E., Czaplinska, A., Dang, C.N., Datta, S., Dee, N.R., Desaki, A.L., Desta, T., Diep, E., Dolbeare, T.A., Donelan, M.J., Dong, H.W., Dougherty, J.G., Duncan, B.J., Ebbert, A.J., Eichele, G., Estin, L.K., Faber, C., Facer, B.A., Fields, R., Fischer, S.R., Fliss, T.P., Frensley, C., Gates, S.N., Glattfelder, K.J., Halverson, K.R., Hart, M.R., Hohmann, J.G., Howell, M.P., Jeung, D.P., Johnson, R.A., Karr, P.T., Kawal, R., Kidney, J.M., Knapik, R.H., Kuan, C.L., Lake, J.H., Laramee, A.R., Larsen, K.D., Lau, C., Lemon, T.A., Liang, A.J., Liu, Y., Luong, L.T., Michaels, J., Morgan, J.J., Morgan, R.J., Mortrud, M.T., Mosqueda, N.F., Ng, L.L., Ng, R., Orta, G.J., Overly, C.C., Pak, T.H., Parry, S.E., Pathak, S.D., Pearson, O.C., Puchalski, R.B., Riley, Z.L., Rockett, H.R., Rowland, S.A., Royall, J.J., Ruiz, M.J., Sarno, N.R., Schaffnit, K., Shapovalova, N.V., Sivisay, T., Slaughterbeck, C.R., Smith, S.C., Smith, K.A., Smith, B.I., Sodt, A.J., Stewart, N.N., Stumpf, K.R., Sunkin, S.M., Sutram, M., Tam, A., Teemer, C.D., Thaller, C., Thompson, C.L., Varnam, L.R., Visel, A., Whitlock, R.M., Wohnoutka, P.E., Wolkey, C.K., Wong, V.Y., et al., 2007. Genome-wide atlas of gene expression in the adult mouse brain. Nature 445, 168–176.

Leterrier, C., Laine, J., Darmon, M., Boudin, H., Rossier, J., Lenkei, Z., 2006. Constitutive activation drives compartment-selective endocytosis and axonal targeting of type 1 cannabinoid receptors. J. Neurosci. Off. J. Soc. Neurosci. 26, 3141–3153.

Luttrell, L.M., Gesty-Palmer, D., 2010. Beyond desensitization: physiological relevance of arrestin-dependent signaling. Pharmacol. Rev. 62, 305–330.

Maurel, D., Comps-Agrar, L., Brock, C., Rives, M.L., Bourrier, E., Ayoub, M.A., Bazin, H., Tinel, N., Durroux, T., Prezeau, L., Trinquet, E., Pin, J.P., 2008. Cell-surface protein-protein interaction analysis with time-resolved FRET and snap-tag technologies: application to GPCR oligomerization. Nat. Methods 5, 561–567.

Mikasova, L., Groc, L., Choquet, D., Manzoni, O.J., 2008. Altered surface trafficking of presynaptic cannabinoid type 1 receptor in and out synaptic terminals parallels receptor desensitization. Proc. Natl. Acad. Sci. U. S. A. 105, 18596–18601.

Morgan, D.J., Davis, B.J., Kearn, C.S., Marcus, D., Cook, A.J., Wager-Miller, J., Straiker, A., Myoga, M.H., Karduck, J., Leishman, E., Sim-Selley, L.J., Czyzyk, T.A.,

Bradshaw, H.B., Selley, D.E., Mackie, K., 2014. Mutation of putative GRK phosphorylation sites in the cannabinoid receptor 1 (CB1R) confers resistance to cannabinoid tolerance and hypersensitivity to cannabinoids in mice. J. Neurosci. Off. J. Soc. Neurosci. 34, 5152–5163.

Niehaus, J.L., Liu, Y., Wallis, K.T., Egertova, M., Bhartur, S.G., Mukhopadhyay, S., Shi, S., He, H., Selley, D.E., Howlett, A.C., Elphick, M.R., Lewis, D.L., 2007. CB1 cannabinoid receptor activity is modulated by the cannabinoid receptor interacting protein CRIP 1a. Mol. Pharmacol. 72, 1557–1566.

Pierce, K.L., Maudsley, S., Daaka, Y., Luttrell, L.M., Lefkowitz, R.J., 2000. Role of endocytosis in the activation of the extracellular signal-regulated kinase cascade by sequestering and nonsequestering G protein-coupled receptors. Proc. Natl. Acad. Sci. U. S. A. 97, 1489–1494.

Quoyer, J., Janz, J.M., Luo, J., Ren, Y., Armando, S., Lukashova, V., Benovic, J.L., Carlson, K.E., Hunt 3rd, S.W., Bouvier, M., 2013. Pepducin targeting the C-X-C chemokine receptor type 4 acts as a biased agonist favoring activation of the inhibitory G protein. Proc. Natl. Acad. Sci. U. S. A. 110, E5088–E5097.

Shenoy, S.K., Modi, A.S., Shukla, A.K., Xiao, K., Berthouze, M., Ahn, S., Wilkinson, K.D., Miller, W.E., Lefkowitz, R.J., 2009. Beta-arrestin-dependent signaling and trafficking of 7-transmembrane receptors is reciprocally regulated by the deubiquitinase USP33 and the E3 ligase Mdm2. Proc. Natl. Acad. Sci. U. S. A. 106, 6650–6655.

Shukla, A.K., Violin, J.D., Whalen, E.J., Gesty-Palmer, D., Shenoy, S.K., Lefkowitz, R.J., 2008. Distinct conformational changes in beta-arrestin report biased agonism at seven-transmembrane receptors. Proc. Natl. Acad. Sci. U. S. A. 105, 9988–9993.

Shukla, A.K., Xiao, K., Lefkowitz, R.J., 2011. Emerging paradigms of beta-arrestin-dependent seven transmembrane receptor signaling. Trends Biochem. Sci. 36, 457–469.

Simon, A.C., Loverdo, C., Gaffuri, A.L., Urbanski, M., Ladarre, D., Carrel, D., Rivals, I., Leterrier, C., Benichou, O., Dournaud, P., Szabo, B., Voituriez, R., Lenkei, Z., 2013. Activation-dependent plasticity of polarized GPCR distribution on the neuronal surface. J. Mol. Cell Biol. 5, 250–265.

Smith, T.H., Blume, L.C., Straiker, A., Cox, J.O., David, B.G., McVoy, J.R., Sayers, K.W., Poklis, J.L., Abdullah, R.A., Egertova, M., Chen, C.K., Mackie, K., Elphick, M.R., Howlett, A.C., Selley, D.E., 2015. Cannabinoid receptor-interacting protein 1a modulates CB1 receptor signaling and regulation. Mol. Pharmacol. 87, 747–765.

Stadel, R., Ahn, K.H., Kendall, D.A., 2011. The cannabinoid type-1 receptor carboxyl-terminus, more than just a tail. J. Neurochem. 117, 1–18.

Staus, D.P., Wingler, L.M., Strachan, R.T., Rasmussen, S.G., Pardon, E., Ahn, S., Steyaert, J., Kobilka, B.K., Lefkowitz, R.J., 2014. Regulation of beta2-adrenergic receptor function by conformationally selective single-domain intrabodies. Mol. Pharmacol. 85, 472–481.

Straiker, A., Wager-Miller, J., Mackie, K., 2012. The CB1 cannabinoid receptor C-terminus regulates receptor desensitization in autaptic hippocampal neurones. Br. J. Pharmacol. 165, 2652–2659.

Techlovska, S., Chambers, J.N., Dvorakova, M., Petralia, R.S., Wang, Y.X., Hajkova, A., Nova, A., Frankova, D., Prezeau, L., Blahos, J., 2014. Metabotropic glutamate receptor 1 splice variants mGluR1a and mGluR1b combine in mGluR1a/b dimers in vivo. Neuropharmacology 86, 329–336.

Tohgo, A., Choy, E.W., Gesty-Palmer, D., Pierce, K.L., Laporte, S., Oakley, R.H., Caron, M.G., Lefkowitz, R.J., Luttrell, L.M., 2003. The stability of the G protein-coupled receptor-beta-arrestin interaction determines the mechanism and functional consequence of ERK activation. J. Biol. Chem. 278, 6258–6267.

Traub, L.M., Wendland, B., 2010. Cell biology: how to don a coat. Nature 465, 556–557.

Trevaskis, J., Walder, K., Foletta, V., Kerr-Bayles, L., McMillan, J., Cooper, A., Lee, S., Bolton, K., Prior, M., Fahey, R., Whitecross, K., Morton, G.J., Schwartz, M.W., Collier, G.R., 2005. Src homology 3-domain growth factor receptor-bound 2-like (endophilin) interacting protein 1, a novel neuronal protein that regulates energy balance. Endocrinology 146, 3757–3764.

Uezu, A., Horiuchi, A., Kanda, K., Kikuchi, N., Umeda, K., Tsujita, K., Suetsugu, S., Araki, N., Yamamoto, H., Takenawa, T., Nakanishi, H., 2007. SGIP1alpha is an endocytic protein that directly interacts with phospholipids and Eps15. J. Biol. Chem. 282, 26481–26489.

Vallee, M., Vitiello, S., Bellocchio, L., Hebert-Chatelain, E., Monlezun, S., Martin-Garcia, E., Kasanetz, F., Baillie, G.L., Panin, F., Cathala, A., Roullot-Lacarriere, V., Fabre, S., Hurst, D.P., Lynch, D.L., Shore, D.M., Deroche-Gamonet, V., Spampinato, U., Revest, J.M., Maldonado, R., Reggio, P.H., Ross, R.A., Marsicano, G., Piazza, P.V., 2014. Pregnenolone can protect the brain from cannabis intoxication. Science 343, 94–98.

Wilhelm, B.G., Mandad, S., Truckenbrodt, S., Krohnert, K., Schafer, C., Rammner, B., Koo, S.J., Classen, G.A., Krauss, M., Haucke, V., Urlaub, H., Rizzoli, S.O., 2014. Composition of isolated synaptic boutons reveals the amounts of vesicle trafficking proteins. Science 344, 1023–1028.